IEEE Access
Multidisciplinary | Rapid Review | Open Access Journal

Received April 26, 2021, accepted May 11, 2021, date of publication May 14, 2021, date of current version May 24, 2021.

*Digital Object Identifier 10.1109/ACCESS.2021.3080576*

# First Quantization Estimation by a Robust Data Exploitation Strategy of DCT Coefficients

**SEBASTIANO BATTIATO[1], (Senior Member, IEEE), OLIVER GIUDICE[1], FRANCESCO GUARNERA[1], (Student Member, IEEE), AND GIOVANNI PUGLISI[2]**

[1]Dipartimento di Matematica e Informatica, University of Catania, 95125 Catania, Italy
[2]Dipartimento di Matematica e Informatica, University of Cagliari, 09124 Cagliari, Italy

Corresponding author: Oliver Giudice (giudice@dmi.unict.it)

**ABSTRACT** It is well known that the JPEG compression pipeline leaves residual traces in the compressed images that are useful for forensic investigations. Through the analysis of such insights the history of a digital image can be reconstructed by means of First Quantization Estimations (FQE), often employed for the camera model identification (CMI) task. In this paper, a novel FQE technique for JPEG double compressed images is proposed which employs a mixed approach based on Machine Learning and statistical analysis. The proposed method was designed to work in the aligned case (i.e., $8 \times 8$ JPEG grid is not misaligned among the various compressions) and demonstrated to be able to work effectively in different challenging scenarios (small input patches, custom quantization tables) without strong a-priori assumptions, surpassing state-of-the-art solutions. Finally, an in-depth analysis on the impact of image input sizes, dataset image resolutions, custom quantization tables and different Discrete Cosine Transform (DCT) implementations was carried out.

**INDEX TERMS** FQE, JPEG, multimedia forensics.

## I. INTRODUCTION

The everyday number of digital images acquired, stored or simply shared is constantly growing due to the widespread of social networks. Similarly to other kind of data, it is possible to give a life-cycle to digital images, consisting on the following steps: acquisition by means of a digital device, editing and uploading to Instant Messaging platforms or Social Networks (these last steps could be done more than once). Often, the aforementioned steps, produce a JPEG double (multiple) compression [1] on the image data, which means that a lot of the original information (acquisition) is definitively lost. If the image became a forensic evidence it would be investigated: its history needs to be reconstructed ([2], [3]). This reconstruction could be done by identifying, whenever is possible, the camera model and the camera source device [4], [5]. Specifically the investigation process would start by detecting traces of the double compression [6], then go through the retrieval of the camera model by means of First Quantization Estimation (FQE) [7] and finally the identification of the source by means of Photo Response Non Uniformity (PRNU) analysis ([4], [8]). In this paper, a novel approach for the estimation of quantization factors is presented. In order to estimate the quantization factors employed in the first quantization matrix in images JPEG double compressed, the proposed approach exploits comparisons with a proper reference dataset of distributions built on Discrete Cosine Transform (DCT) statistics [9]. Specifically, the proposed method was designed to cope with the typical limits affecting both statistical FQE approaches (e.g., low accuracy with small patches, strong a-priori assumptions about involved quantization matrices) and machine learning based methods (e.g., overfitting with respect to input patch content and quantization tables employed in the training phase). It works without strong a-priori assumptions on the quantization matrices employed in the compression process of the analysed images.

Although some state-of-the-art methods ([10], [11]) employed more complex properties and modeling of the DCT distributions, these are not employed in the presented work due to computational limits. Experimental results in challenging scenarios (i.e., small patches, custom quantization tables) and comparisons with the state-of-the-art, demonstrated the effectiveness of the proposed method. A preliminary version of the technique was proposed in [12]. In this paper, the experimental part was widely extended with an in-depth

The associate editor coordinating the review of this manuscript and approving it for publication was Yizhang Jiang.

analysis of the performances of the method at varying of input patch sizes, employed datasets (low and high resolution), different DCT implementations.

The remainder of this paper is organized as in the following. In Section II the state-of-the-art is presented; Section III explains the JPEG notation employed in the paper; Section IV describes the proposed novel approach with discussion on its parameters in Section V. Experimental results are reported in Section VI while Section VII concludes the paper.

## II. RELATED WORKS

First quantization estimation is extremely useful when conducting forensic investigations as it gives information about the history of images. In recent years several solutions have been proposed. The research activity on the field was mainly devoted, at first, to the estimation of the first quantization factors when a change of image file format (e.g., from JPEG to Bitmap), is involved in the process. Fan and De Queiroz in [3] outlined a method to detect whether a Bitmap image was previously JPEG compressed and subsequently estimated the applied quantization matrix; the same scenario with different lossless formats is faced by Li *et al.* [13]. The problem was firstly studied in a simpler single compression and file format change scenario useful to understand the produced JPEG artifacts. This attracted the attention of more researchers: to date [14]. Bianchi and Piva [15], Bianchi *et al.* [16], and Piva and Bianchi [17] proposed the first robust technique for FQE; based on the Expectation Maximization algorithm to determine the most likely quantization factors for the primary compression over a set of candidates.

Histograms of the quantized DCT coefficients have been analyzed in different ways. Galvan *et al.* [18] introduced a technique that worked only at specific conditions. Similar approaches related to histogram analysis and filtering have been introduced in [19], [20] and [21] while others techniques faced the task with high resolution images [22]. More recently, the intuitive insights employed for steganography detection have been exploited by Thai *et al.* ([10], [23]). Although they have obtained good results in terms of overall accuracy, their method only worked with specific first-second compression factor combinations, avoiding estimation when multiple quantization factors are involved. Given the large amount of data that can be computationally analyzed today, such issue has been also addressed by means of modern Machine Learning approaches. Lukáš and Fridrich in [24] have provided an initial tentative by exploiting neural networks, further refined in [25] with error considerations similar to [18]. Recently, some papers ([26]–[28]) have faced the FQE problem through the use of Convolutional Neural Networks (CNNs). CNNs have proven to be amazingly strong at spotting undetectable correlations on data, however, due to the large number of involved parameters, they could suffer from overfitting (i.e., the obtained model is not generalizable enough to represent the phenomenon under analysis).

Machine Learning techniques such as CNNs may be closely related to the dataset they were trained on. The reliability of these methods need then to be demonstrated under ''wild'' conditions. State-of-the-art CNN results have been achieved by Niu *et al.* [29] and Tondi *et al.* [30] where the best results for both aligned and non-aligned FQE scenarios were presented.

The proposed method, employing a minimal set of parameters and a reference dataset, is designed to overcome the limitations of both CNN-based and analytical state-of-the-art solutions. This may be accomplished by fitting appropriate statistics on DCT coefficients in order to get rid of the necessity of a training phase and without falling into all those limitations of an analytical methods.

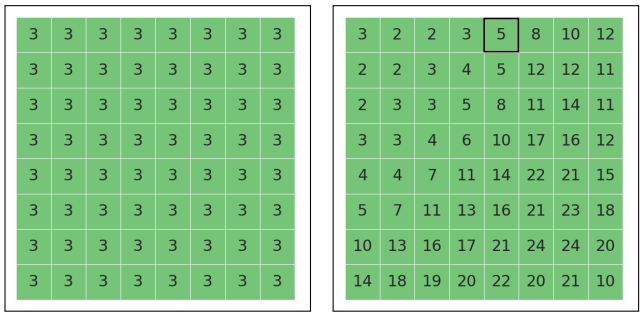


a. $M_i$ b. Standard matrix $QF = 90$

**FIGURE 1. Example of the constant matrix $M_i$ with $i = 3$ (a), and the standard quantization matrix with $QF = 90$ (b).**

## III. JPEG NOTATION

Starting from a raw image $I$, JPEG compression [31] could be defined as a function $f_Q$ such that $I' = f_Q(I)$, where $I'$ is the JPEG compressed image, $Q$ is a $8 \times 8$ quantization matrix composed by the quantization factors $q_i \in \mathbb{N}$ with $i \in \{1, 2, \ldots, 64\}$. Firstly, $f_Q(I)$ converts $I$ from the RGB color space to the YCbCr one, then divides it in $8 \times 8$ non-overlapping blocks and applies the integer DCT. Finally, each $8 \times 8$ block is divided by $Q$ pixel by pixel, rounded (losing information) and then encoded by classic entropy based engine. In the analysis presented in this paper, only Y channel (luminance) will be considered. Let's define $I'' = f_{Q_2}(f_{Q_1}(I))$ a JPEG double compressed image, where $Q_1$ and $Q_2$ are the quantization matrices employed for the first and the second compression respectively.

In this paper, we will refer to $QF$ as the standard quantization matrix defined by JPEG for a specific quality factor [31]. $QF_i$ denotes the quality factor used for the $i$-th JPEG compression.

We denote with $h_i$ the empirical distributions built from the $i$-th DCT coefficients considering all the $8 \times 8$ blocks of $I''$. Moreover, we define the $k$ quantization factors in zig-zag order of $Q_1$ as $q1_1, q1_2, \ldots, q1_k$, and the quantization factors employed in the first and in the second compression as $q1$ and $q2$. Finally, in our tests, we define $q1_{max}$ as the maximum value among all the quantization factors to be predicted. Considering as example the matrix reported in Fig. 1b and $q1_1, q1_2, \ldots, q1_k$ in zig-zag order with $k = 15$, $q1_{max}$ value is 5 (highlighted in the figure).

## IV. FQE THROUGH COMPARISON

### A. RETRIEVAL DISTRIBUTIONS

The proposed solution aims to exploit the information available in double JPEG compressed images without suffering from overfitting that usually limits Machine Learning approaches. In the state-of-the-art, many FQE methods point out some limits with respect to the specific quantization tables on which they work; for example Niu *et al.* in [29] and Tondi *et al.* in [30] provide Neural Network models only trained with standard quantization matrices as $Q_2$ (with $QF_2 \in \{80, 90\}$). To this aim, an additional contribution of our method is the ability to provide satisfactory results even in challenging conditions (i.e., custom matrices) where other methods typically fail.

The first part of the underlying technique is the generation of the reference data to compare with the query image for the FQE. To this purpose, starting from a collection of 8156 high-resolution uncompressed images (RAISE dataset [33]) a $64 \times 64$ central patch was extracted. Then, every combination of constant matrix $M_i$ (Fig. 1), with $i \in \{1, 2, \ldots, q1_{max}\}$ was employed for the double compression of the image. The choice of $q1_{max}$ has been done taking into account realistic scenarios as detailed in the following. We observed a good trade-off between the amount of the data to be generated ($q1_{max} \times q1_{max}$ combinations) and the maximum quantization factor to be estimated. Taking into account the standard quantization tables, $q1_{max} = 22$ (in the first $k = 15$ DCT coefficients) means including all the standard matrices with $QF \geq 55$ which represents the worst case usually analyzed for this scenario in the state-of-the-art. Moreover, if we consider the collection of matrices employed in real-case-scenario as those shown in Park *et al.* [32] it means considering about the 81% of them (873 on 1070) (Fig. 3).

Hence, we generated $8156 \times 22 \times 22 = 3.947.504$ double compressed images. The generated dataset represents the set of items considered for the comparisons. The choice to build the reference dataset employing the combinations of constant matrices $M_i$ was done in order to safely break the correlation with real quantization matrices (e.g., standard ones). This composition makes generalizable the approach w.r.t. any JPEG double compressed image (in the aligned scenario). To carry out the comparison between the query item (JPEG double compressed image under analysis) and the reference dataset, DCT coefficient distributions $h_i$, with $i \in 1, 2, \ldots, q1_{max}$ were employed. For this reason, the first $k$ distributions $h_i$ were calculated, and then clustered in sub-datasets labelled by the couple $\{q1, q2\}$.

Lam and Goodman [9] have shown the usefulness of the Laplacian distribution (1) during the years ([34], [35]); we then fitted the distributions $h_i$ of ACs by considering the following equation:

$$f(x) = \frac{1}{2\beta} \exp\left(\frac{-|x - \mu|}{\beta}\right) \tag{1}$$

where $\beta$ and $\mu$ are obtained through MLE (Maximum Likelihood Estimation) closed form solution.

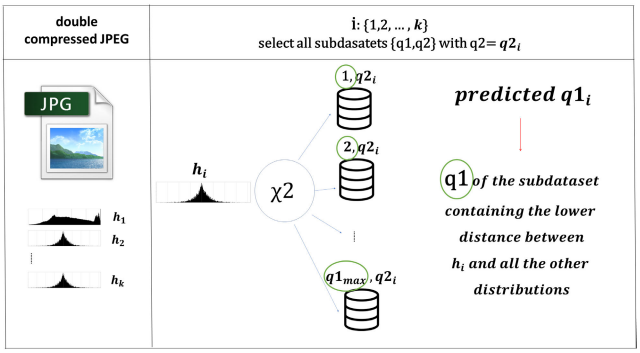


**FIGURE 2.** A schematic representation of the proposed FQE method. The pipeline starts with a JPEG double compressed image. Each DCT histogram $h_i$ is then compared with proper subdatasets computing $\chi^2$ distance. Most similar histogram for each element is chosen for the FQE task.

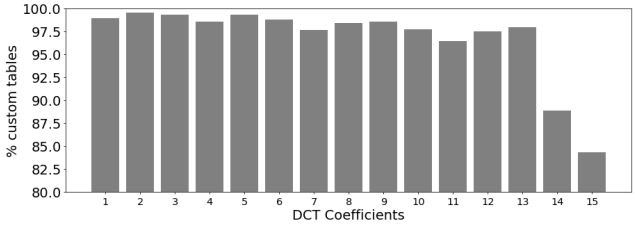


**FIGURE 3.** Percentages of custom matrices in Park's dataset [32] with quantization factors lower than 23 for the first 15 coefficients.

The estimation of $\beta$ was employed for sub-datasets sorting of the AC distributions ($h_i$ with $i > 1$), while the sort of DC distributions $h_1$ was done through the use of median value $m$. The reference dataset after sorting is composed as follows:

- $DC_{dset}$: $DC$ distributions split for every possible couple $\{q1, q2\}$ sub-datasets (sorted by $m$);
- $AC_{dset}$: $AC$ distributions split for every possible couple $\{q1, q2\}$ sub-datasets (sorted by $\beta$).

The model described in (1) is very simple and allows to better organize the data reducing at the same time the computational complexity of the proposed solution. For this reason more complex models, as in [10], are not required here. It is clear that the performance of the algorithm has a little dependence with the training set: bigger is the training set, better will be the estimation. The overall dimensions of involved datasets in our experiments have been selecting accordingly.

### B. QUANTIZATION FACTOR ESTIMATION

Given $I''$, the estimation of the first $k$ quantization factors $\{q1_1, q1_2, \ldots, q1_k\}$ of $Q_1$ is summarized in Algorithm 1 and Figure 2.

Every single $q1_i$ with $i \in \{1, 2, \ldots, k\}$ is estimated through the following steps:

1) extract $h_i$ from $I''$ employing LibJpeg C library.[1]
2) fit $h_i$ to the Laplacian distribution in order to extract $\beta$ (if $i > 1$) or compute the median value $m$ (if $i = 1$).

[1] https://github.com/LuaDist/libjpeg

**Algorithm 1** The Proposed FQE Technique

**Input:** double compressed image $I''$
**Output:** $\{q1_1, q1_2, \ldots, q1_k\}$
*Initialization* : $k$, $q1_{max}$
**for** $i = 1$ to $k$ **do**
  $h_i$ : (empirical) distribution of $i$-th DCT coefficient
  **if** $(i = 1)$ **then**
    $D : DC_{dset}$
    $m$ : median value of $h_i$
  **else**
    $D : AC_{dset}$
    $\beta$ : $\beta$ fitted on Laplacian $h_i$
  **end if**
  $q2_i$ : quantization factor of $Q_2$ for $i$-th DCT
  **for** $j = 1$ to $q1_{max}$ **do**
    $D_{j,q2_i}$ : sub-dataset $(q1, q2)$ with $q1 = j, q2 = q2_i$
    $D_{j,q2_i}(m, \beta)$ : sub-range with most similar $m$, $\beta$
    $d_{i,j}$ : lower $\chi^2$ distance between $h_i$ and $D_{j,q2_i}$
  **end for**
  $q1_i$ : $\arg\min_{\{d_{i,j}\}}, j \in \{1, 2, \ldots, q1_{max}\}$
**end for**
regularize($\{q1_1, q1_2, \ldots, q1_k\}$)
**return** $\{q1_1, q1_2, \ldots, q1_k\}$

3) use $\beta$ (or $m$) to seek the range of candidates from the reference dataset.
4) find the most similar distribution between the candidates.

It is worth noting that the step 1 avoids further truncation and rounding errors and the usage of $\beta$ (if $i > 1$) and $m$ (if $i = 1$) make constant the computational time to retrieve the most similar distribution.

The header of a JPEG file contains the matrix employed in the last compression, $Q_2$ in the considered scenario. The availability of $q2_i$ allows us to select the sub-dataset to be employed. For each sub-dataset $\{q_j,q2_i\}$ with $j \in \{1, 2, \ldots, q1_{max}\}$ we select a range of elements $D_{j,q2_i}(m, \beta)$ with the most similar values of $\beta$ for $AC_{dset}$ and $m$ for $DC_{dset}$, to be compared with $h_i$ using $\chi^2$ distance:

$$\chi^2(x, y) = \sum_{i=1}^{m} (x_i - y_i)^2/(x_i + y_i) \tag{2}$$

where $x$ and $y$ are the distributions to compare.

Given a sub-dataset $D_{j,q2_i}$, we select the lowest distance $d_{i,j}$ obtaining $q1_{max}$ distances. The minimum distance $d_{i,j}$, $j \in \{1, 2, \ldots, q1_{max}\}$ allows to find the related sub-dataset and then the predicted $q1$ for the current $i$.

### C. REGULARIZATION

Analyzing the distances $d_{i,j}$ obtained in the previous section, it is possible to note that a strong minimum cannot be always found. Sometimes, the histogram $h_i$ does not contains enough information to discriminate among the $q1_i$ values to be estimated. In order to overcome such limitation, also data related to neighboring DCT coefficients have been considered. Specifically, the empirical hypothesis that consecutive first quantization factors considered in zig-zag order have similar values has been exploited. Taking into account three consecutive $q1$, and fixed $k = 15$, 13 triplets ($q1_{i-1}$, $q1_i$, $q1_{i+1}$, $i = 2, \ldots, 14$) can be found. A single triplet ($q1_{i-1}$, $q1_i$, $q1_{i+1}$) can be then estimated through a cost function in which all possible $q1$ combinations (i.e., $22 \times 22 \times 22$ with $q1_{max} = 22$) are considered. The cost function $C$ is designed as the weighted average of a data term ($C_{data}$) and a regularization term ($C_{reg}$):

$$C = wC_{data} + (1 - w)C_{reg} \tag{3}$$

where $w \in [0, 1]$, $C_{data}$ is the normalized sum of the three distances $d_{i,j}$, and $C_{reg}$ is the regularization term introduced to reduce the difference among neighboring $q1$ values. Additional details related to the design of $C_{reg}$ will be presented in Section V-B.

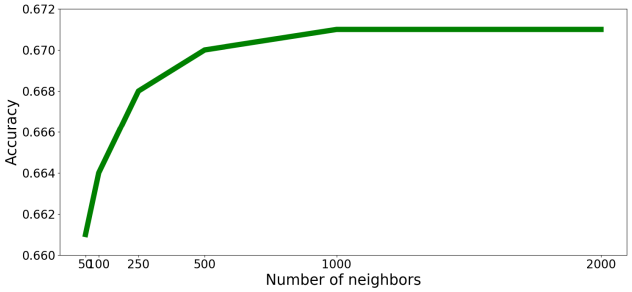


**FIGURE 4.** Accuracy of the proposed approach w.r.t. the number of neighbors considered for comparison.

## V. PARAMETER SETTING

The parameters discussed in Section IV, were set through a validation dataset $D_V$ composed of 8156 $64 \times 64$ pixel patched, cropped at random position from RAISE [33] dataset. For computational reasons, only for the AC coefficients, we employed 1/8 of the available distributions to compose $AC_{dset}$.

### A. CLUSTERING

Given a second quantization factor $q2$, the number of the associated reference sub-dataset to be considered is $q1_{max}$. To reduce the computational complexity of the proposed solution we employed a comparison strategy that properly exploit $m$ and $\beta$ values to limit the number of distributions $h_i$ to be taken into account. To set the right number of comparisons to be performed a sub-range of 50, 100, 250, 500, 1000, 2000 elements for each sub-dataset were tested as shown in Fig. 4. It is evident from the Fig. 4 that the chosen value (i.e., 1000) is a good trade-off between the overall computational cost and the accuracy w.r.t. the full search solution.

### B. REGULARIZATION

As already mentioned in Section IV, sometimes histograms $h_i$ do not contains enough information to properly estimate the related first quantization factors. To cope with this problem a regularization function has been employed. Specifically, the

**TABLE 1.** Accuracies obtained by the proposed approach compared to Bianchi *et al.* [15], Galvan *et al.* [18], Dalmia and Okade [19], Niu *et al.* [29], Tondi *et al.* [30] and Battiato *et al.* [36] with different combinations of $QF_1/QF_2$, considering standard quantization tables.

| $QF_1$ | $QF_2 = 90$ | | | | | | | | $QF_2 = 80$ | | | | | | | |
|---|---|---|---|---|---|---|---|---|---|---|---|---|---|---|---|---|
| | *Our* | *Our Reg.* | *[15]* | *[18]* | *[19]* | *[29]* | *[30]* | *[36]* | *Our* | *Our Reg.* | *[15]* | *[18]* | *[19]* | *[29]* | *[30]* | *[36]* |
| 55 | 0.76 | **0.77** | 0.53 | 0.52 | 0.45 | 0.00 | 0.00 | 0.62 | 0.55 | **0.58** | 0.36 | 0.37 | 0.37 | 0.24 | 0.52 | 0.49 |
| 60 | **0.82** | **0.82** | 0.53 | 0.56 | 0.47 | 0.64 | 0.53 | 0.66 | 0.55 | **0.60** | 0.27 | 0.37 | 0.38 | 0.50 | 0.31 | 0.47 |
| 65 | 0.79 | **0.81** | 0.54 | 0.57 | 0.49 | 0.54 | **0.81** | 0.68 | **0.68** | 0.65 | 0.19 | 0.41 | 0.43 | 0.31 | 0.38 | 0.52 |
| 70 | **0.85** | **0.85** | 0.43 | 0.57 | 0.51 | 0.66 | 0.66 | 0.70 | 0.67 | **0.75** | 0.19 | 0.50 | 0.49 | 0.50 | 0.70 | 0.66 |
| 75 | 0.83 | 0.85 | 0.41 | 0.63 | 0.53 | 0.77 | **0.93** | 0.75 | 0.48 | 0.56 | 0.07 | 0.56 | 0.45 | 0.15 | **0.58** | 0.47 |
| 80 | 0.81 | **0.83** | 0.29 | 0.61 | 0.45 | 0.81 | 0.67 | 0.75 | **0.12** | 0.11 | 0.00 | 0.00 | 0.00 | 0.00 | 0.04 | 0.04 |
| 85 | 0.78 | 0.85 | 0.14 | 0.74 | 0.36 | 0.81 | **0.88** | 0.72 | 0.28 | **0.34** | 0.19 | 0.00 | 0.00 | 0.04 | 0.14 | 0.31 |
| 90 | **0.30** | 0.24 | 0.00 | 0.00 | 0.00 | 0.02 | 0.02 | 0.23 | 0.16 | 0.19 | 0.06 | 0.00 | 0.00 | **0.48** | 0.37 | 0.21 |
| 95 | 0.44 | 0.52 | 0.11 | 0.00 | 0.00 | **0.78** | 0.68 | 0.40 | 0.27 | 0.30 | 0.00 | 0.00 | 0.00 | **0.95** | 0.37 | 0.19 |
| 98 | 0.49 | 0.57 | 0.00 | 0.00 | 0.00 | 0.76 | **0.91** | 0.41 | 0.42 | 0.42 | 0.01 | 0.00 | 0.00 | 0.21 | **0.48** | 0.19 |
| MEAN | 0.69 | **0.71** | 0.30 | 0.42 | 0.33 | 0.58 | 0.61 | 0.59 | 0.42 | **0.45** | 0.13 | 0.22 | 0.21 | 0.28 | 0.39 | 0.36 |

**TABLE 2.** Accuracies obtained by the proposed approach compared to Bianchi *et al.* [15], Galvan *et al.* [18], Niu *et al.* [29], Tondi *et al.* [30] and Battiato *et al.* [36] employing custom tables for first compression. The column *PS* refers to custom tables used by Photoshop.

| $PS$ | $QF_2 = 90$ | | | | | | | $QF_2 = 80$ | | | | | | |
|---|---|---|---|---|---|---|---|---|---|---|---|---|---|---|
| | *Our* | *Our Reg.* | *[15]* | *[18]* | *[29]* | *[30]* | *[36]* | *Our* | *Our Reg.* | *[15]* | *[18]* | *[29]* | *[30]* | *[36]* |
| 5 | **0.80** | 0.78 | 0.56 | 0.58 | 0.05 | 0.10 | 0.69 | 0.65 | **0.68** | 0.26 | 0.46 | 0.07 | 0.08 | 0.57 |
| 6 | **0.82** | **0.82** | 0.46 | 0.60 | 0.07 | 0.13 | 0.75 | 0.42 | **0.54** | 0.05 | 0.41 | 0.02 | 0.06 | 0.42 |
| 7 | **0.83** | **0.83** | 0.41 | 0.58 | 0.07 | 0.09 | 0.70 | 0.62 | **0.68** | 0.15 | 0.48 | 0.08 | 0.10 | 0.56 |
| 8 | **0.81** | **0.81** | 0.25 | 0.65 | 0.10 | 0.13 | 0.74 | 0.19 | **0.22** | 0.03 | 0.03 | 0.01 | 0.04 | 0.18 |
| 9 | 0.55 | **0.61** | 0.02 | 0.47 | 0.02 | 0.05 | 0.47 | 0.26 | **0.28** | 0.19 | 0.00 | 0.07 | 0.13 | **0.28** |
| 10 | 0.42 | **0.50** | 0.19 | 0.00 | 0.25 | 0.33 | 0.43 | 0.15 | 0.20 | 0.00 | 0.00 | **0.40** | 0.16 | 0.17 |
| 11 | 0.45 | 0.52 | 0.04 | 0.00 | 0.69 | **0.75** | 0.40 | 0.37 | **0.38** | 0.01 | 0.00 | 0.24 | **0.38** | 0.23 |
| 12 | 0.49 | 0.57 | 0.04 | 0.00 | 0.75 | **0.85** | 0.41 | 0.42 | 0.42 | 0.01 | 0.00 | 0.21 | **0.44** | 0.26 |
| MEAN | 0.64 | **0.68** | 0.25 | 0.36 | 0.25 | 0.30 | 0.58 | 0.39 | **0.42** | 0.09 | 0.18 | 0.17 | 0.14 | 0.33 |

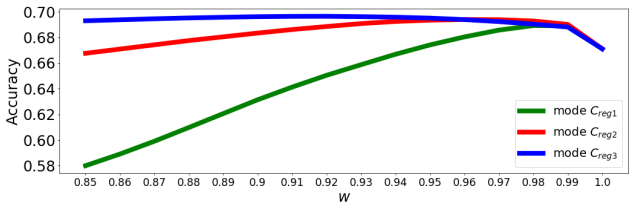


**FIGURE 5.** Comparison between the modes of the accuracies obtained for different values of the regularization parameter $w$ employing the three equations (4), (5), (6) respectively.

proposed approach simultaneously estimates triplets of nearest $q1_i$ and the following $C_{reg}$ functions have been analyzed:

$$C_{reg1} = \frac{|c_i - c_{i-1}| + |c_i - c_{i+1}|}{2} \tag{4}$$

$$C_{reg2} = \frac{|c_i - c_{i-1}| + |c_i - c_{i+1}|}{2\sqrt{c_i}} \tag{5}$$

$$C_{reg3} = \frac{|c_i - c_{i-1}| + |c_i - c_{i+1}|}{2c_i} \tag{6}$$

where $c_{i-1}$, $c_i$, $c_{i+1}$ are consecutive quantization factors candidates in zig-zag order. For each $q1_i$ multiple estimations are actually provided. As example $q1_3$ can be estimated in three different triplets: ($q1_1$, $q1_2$, $q1_3$), ($q1_2$, $q1_3$, $q1_4$) and ($q1_3$, $q1_4$, $q1_5$). Different strategies have been analyzed to properly exploit the information provided by the multiple estimations. As reported in Fig. 5, we studied the modes of multiple estimations related to eq. (4), (5), (6), choosing eq. (6) with $w = 0.92$. The usage of just 3 terms has been selected as a good trade-off in order to characterize local coherence and limit the overall number of requested tests involved in the parameter setting.

## VI. EXPERIMENTAL RESULTS

The difficulty of the first quantization factor estimation task is proportional to the relative position in the quantization matrix, as reported in literature. High frequencies are used to be quantizated heavily and after certain values the recovered value after dequantization is always zero (e.g., 'dead zone' quantization). For this reason but also for comparison with the state-of-the-art, we set $k = 15$, although our method doesn't suffer from this specific limitation on $k$ value.

### A. COMPARISON TESTS

In order to compare the proposed method with state-of-the-art approaches we consider methods based on statistical analysis (Bianchi *et al.* [15], Galvan *et al.* [18], Dalmia *et al.* [19], Battiato *et al.* [36]) and two methods based on Machine Learning (Niu *et al.* [29] and Tondi *et al.* [30]). All the tests were done employing the implementations provided by the authors. In order to carry out the comparisons, 4 different datasets were generated: from every image of RAISE [33] dataset, a random patch 64 × 64 was cropped and then compressed two times by considering:

1) $QF_1 \in \{55, 60, 65, 70, 75, 80, 85, 90, 95, 98\}$, $QF_2 = 90$
2) $QF_1 \in \{55, 60, 65, 70, 75, 80, 85, 90, 95, 98\}$, $QF_2 = 80$
3) $Q_1 \in \{5, 6, 7, 8, 9, 10, 11, 12\}$, $QF_2 = 90$
4) $Q_1 \in \{5, 6, 7, 8, 9, 10, 11, 12\}$, $QF_2 = 80$

where $Q_1 \in \{5, 6, 7, 8, 9, 10, 11, 12\}$ of 3) and 4) are referred to Photoshop's quantization matrices (CC version 20.0.4). All the methods were tested with the datasets described above; only Dalmia *et al.* [19] was excluded in the tests with

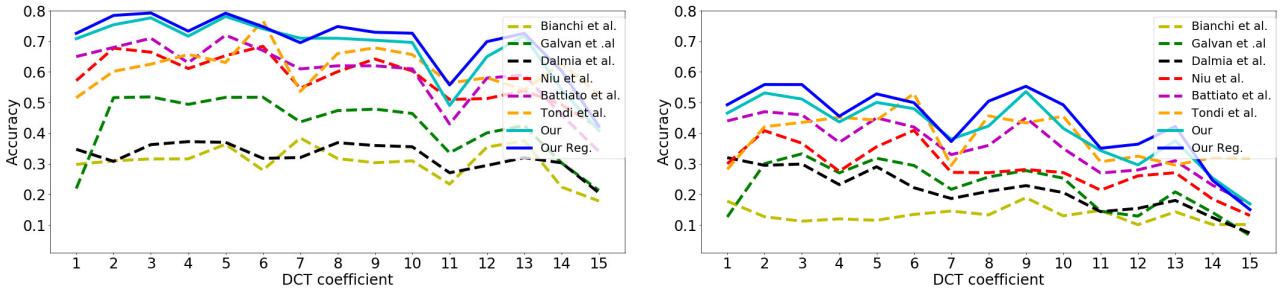


a. $QF_1 \in \{55, 60, 65, 70, 75, 80, 85, 90, 95, 98\}$, $QF_2 = 90$

b. $QF_1 \in \{55, 60, 65, 70, 75, 80, 85, 90, 95, 98\}$, $QF_2 = 80$

c. $Q_1 \in \{5, 6, 7, 8, 9, 10, 11, 12\}$, $QF_2 = 90$

d. $Q_1 \in \{5, 6, 7, 8, 9, 10, 11, 12\}$, $QF_2 = 80$

**FIGURE 6.** Accuracies of the same methods described in Table 1 and 2 at varying of the quantization factors $q1_i$ to be predicted. The values are averaged over all the $QF_1/Q_1$.

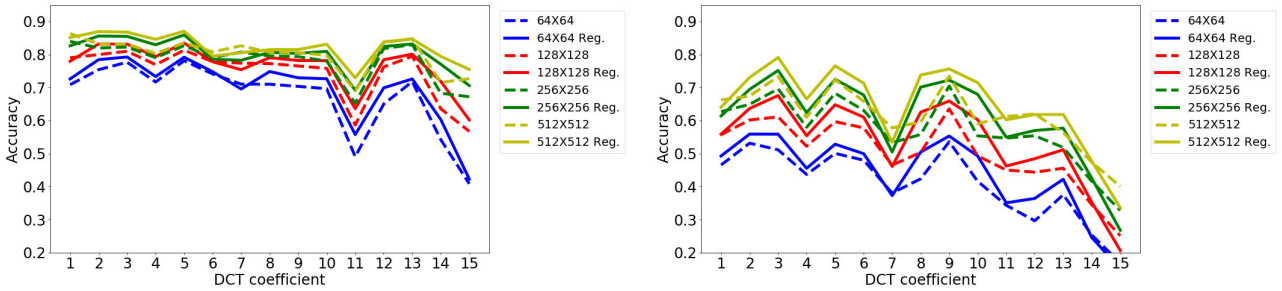


a. $QF_1 \in \{55, 60, 65, 70, 75, 80, 85, 90, 95, 98\}$, $QF_2 = 90$

b. $QF_1 \in \{55, 60, 65, 70, 75, 80, 85, 90, 95, 98\}$, $QF_2 = 80$

c. $Q_1 \in \{5, 6, 7, 8, 9, 10, 11, 12\}$, $QF_2 = 90$

d. $Q_1 \in \{5, 6, 7, 8, 9, 10, 11, 12\}$, $QF_2 = 80$

**FIGURE 7.** Accuracies of the proposed method at varying of training/test patch size. The values are averaged over all $QF_1/Q_1$.

Photoshop's custom tables (datasets 3 and 4) because the related implementation makes assumptions about standard tables employed in the first compression.

As reported in Table 1, 2 and Fig. 6 the proposed approach outperforms state-of-the-art methods in almost all scenarios (values close to 0 are due to the assumptions of some methods, e.g., $QF_1 < QF_2$). Note that the regularization step improves the results in almost all cases. Moreover, although the standard matrices scenario (Table 1) is the one considered by Tondi *et al.* [30] to train their CNN, the proposed method outperforms it (0.71 vs. 0.59 for $QF_2 = 90$ and 0.45 vs. 0.37 for $QF_2 = 80$) in almost all cases. Results reported in Table 2 involving Photoshop's custom tables demonstrates that the proposed method, differently than other Machine Learning

**TABLE 3.** Accuracies of the proposed approach for generalizing property demonstration (Our Reg. denotes the regularized version). It is worth noting that, given a patch size $N \times N$, the same dataset was employed as reference (i.e., RAISE $N \times N$) for both input (i.e., RAISE $N \times N$, UCID $N \times N$).

| Method | Test Dataset | Cropped Patch | Low/Low | Low/Mid | Low/High | Mid/Low | Mid/Mid | Mid/High | High/Low | High/Mid | High/High | Mean |
|---|---|---|---|---|---|---|---|---|---|---|---|---|
| Our | RAISE [33] | 64 × 64 | 0.25 | 0.47 | 0.79 | 0.17 | 0.32 | 0.82 | **0.27** | 0.31 | 0.70 | 0.46 |
| Our Reg. | | | **0.30** | **0.53** | **0.81** | **0.22** | **0.37** | **0.84** | 0.25 | **0.33** | **0.75** | **0.49** |
| Our | UCID [37] | 64 × 64 | 0.33 | 0.63 | 0.93 | 0.20 | 0.39 | 0.90 | **0.15** | 0.21 | 0.66 | 0.49 |
| Our Reg. | | | **0.36** | **0.65** | **0.96** | **0.23** | **0.42** | **0.91** | 0.13 | **0.23** | **0.73** | **0.51** |
| Our | RAISE [33] | 128 × 128 | 0.36 | **0.60** | 0.85 | 0.29 | 0.44 | 0.87 | **0.25** | 0.32 | 0.74 | 0.52 |
| Our Reg. | | | **0.41** | 0.55 | **0.88** | **0.34** | **0.48** | **0.89** | **0.25** | **0.38** | **0.79** | **0.55** |
| Our | UCID [37] | 128 × 128 | 0.47 | 0.76 | 0.96 | 0.31 | 0.49 | **0.94** | 0.18 | 0.29 | 0.74 | 0.57 |
| Our Reg. | | | **0.50** | **0.79** | **0.96** | **0.35** | **0.51** | 0.93 | **0.20** | **0.34** | **0.79** | **0.60** |
| Our | RAISE [33] | 256 × 256 | 0.45 | 0.69 | 0.88 | 0.38 | 0.52 | 0.89 | 0.25 | 0.36 | 0.77 | 0.58 |
| Our Reg. | | | **0.49** | **0.73** | **0.90** | **0.40** | **0.55** | **0.90** | **0.30** | **0.45** | **0.82** | **0.62** |
| Our | UCID [37] | 256 × 256 | 0.56 | 0.83 | **0.98** | 0.44 | 0.57 | **0.96** | 0.23 | 0.34 | 0.77 | 0.63 |
| Our Reg. | | | **0.60** | **0.85** | 0.97 | **0.48** | **0.60** | **0.96** | **0.28** | **0.43** | **0.82** | **0.67** |
| Our | RAISE [33] | 512 × 512 | **0.50** | 0.74 | 0.91 | 0.44 | 0.57 | 0.91 | 0.26 | 0.38 | 0.77 | 0.61 |
| Our Reg. | | | **0.50** | **0.78** | **0.92** | **0.48** | **0.59** | **0.92** | **0.32** | **0.48** | **0.83** | **0.65** |
| Our | UCID [37] | Full size | 0.63 | 0.86 | **0.98** | 0.51 | **0.62** | **0.96** | 0.27 | 0.39 | 0.80 | 0.66 |
| Our Reg. | | | **0.67** | **0.87** | 0.97 | **0.56** | **0.62** | **0.96** | **0.37** | **0.49** | **0.85** | **0.71** |

**TABLE 4.** Accuracy obtained employing different DCT implementations for JPEG compression. It is worth noting that the different implementation are referred to the test set; the reference dataset is the same employed in the previous tests (i.e., RAISE double compressed images with DCT Pillow implementation).

| | 60 | 65 | 70 | 75 | 80 | 85 | 90 | 95 | **MEAN** |
|---|---|---|---|---|---|---|---|---|---|
| Pillow | 0,86 | 0,83 | 0,88 | 0,87 | 0,86 | 0,79 | 0,31 | 0,42 | **0,73** |
| libjpeg-turbo | 0,85 | 0,82 | 0,87 | 0,85 | 0,83 | 0,77 | 0,32 | 0,42 | **0,72** |

solutions, does not depend on a specific class of quantization matrices.

To further confirm the effectiveness of the proposed solution, additional experiments at varying of patch size have been performed. Specifically, three double compressed training datasets obtained from RAISE with 128 × 128, 256×256, 512×512 patches have been generated. Moreover, test datasets considering the aforementioned patch sizes with standard and custom tables (Photoshop) for $Q_1$ and $QF_2 \in \{80, 90\}$ have been also created. In a nutshell we have considered the same conditions of tests already seen before, but with more informative patches. As can be seen from Fig. 7, due to the higher amount of information, bigger patches achieve higher accuracy in all the considered scenarios (standard and PS quantization tables). These results confirm the studies performed in [36] to correlate informative content of the patch and estimation accuracy.

### B. GENERALIZING PROPERTY

Park *et al.* in [32] collected a dataset of JPEG quantization matrices employed in real scenarios. The collection consists of 1170 different matrices: 1070 custom and 100 standard JPEG quantization tables. This collection can be then exploited to conduct a new series of tests to evaluate the generalization capability of the proposed solution. Specifically, the matrices with $q1_i \leq q1_{max} = 22$ and $i \in \{1, 2, \ldots, 15\}$ (see Section VI) have been selected, sorted by the average of the first 15 quantization factors and then split into three sets of 291 elements (Low, Mid, High). These sets of tables are then employed to create 9 combinations of double compressions. In our test four different patch sizes ($64 \times 64$, $128 \times 128$, $256 \times 256$, $512 \times 512$) have been considered. For each combination of double compression, the quantization tables ($Q_1$ and $Q_2$) are selected randomly from the 291 available in the corresponding set (Low, Mid, High). The results obtained on these tests are reported in Table 3. They clearly show that our method maintains good accuracies on all the tested challenging scenarios demonstrating to achieve same results even when different datasets are employed (e.g., RAISE as reference and UCID as test dataset). The better results with UCID [37] dataset are explainable again with the quantity of information inside it: a 256 × 256 patch extracted from a UCID [37] image (512 × 384) has a quantity of information (of course measured by DCT overall energy)

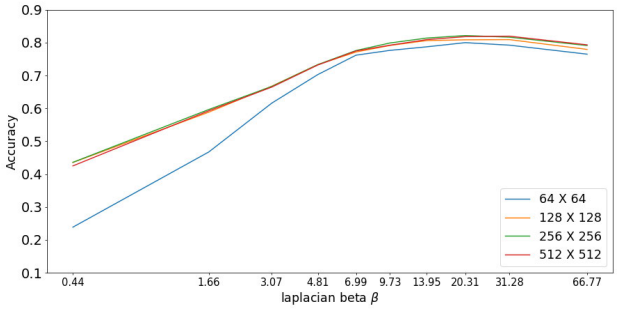


a. Accuracy of RAISE $64 \times 64$ test set at varying of training set

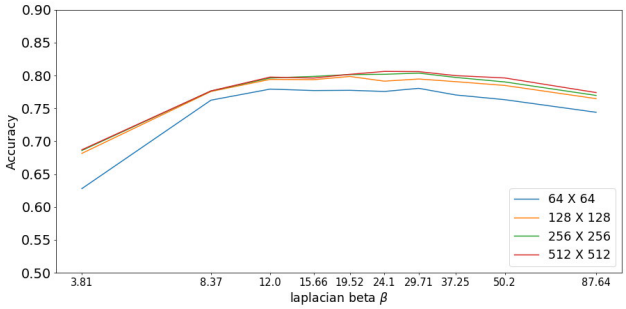


b. Accuracy of UCID $64 \times 64$ test set at varying of training set

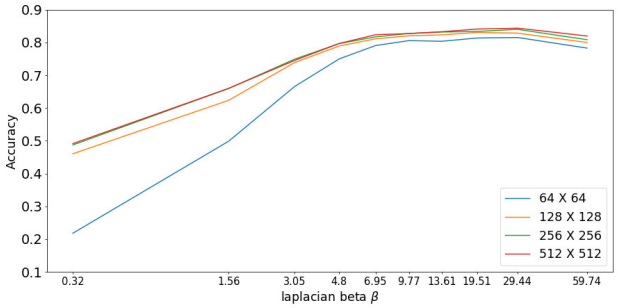


c. Accuracy of RAISE $128 \times 128$ test set at varying of training set

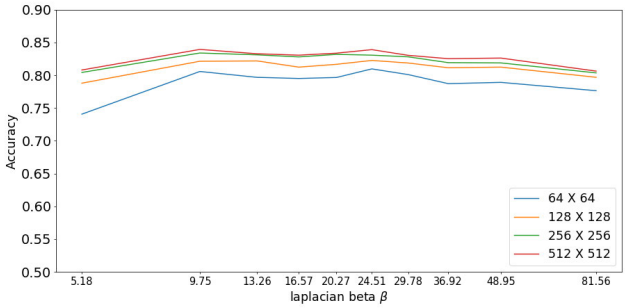


d. Accuracy of UCID $128 \times 128$ test set at varying of training set

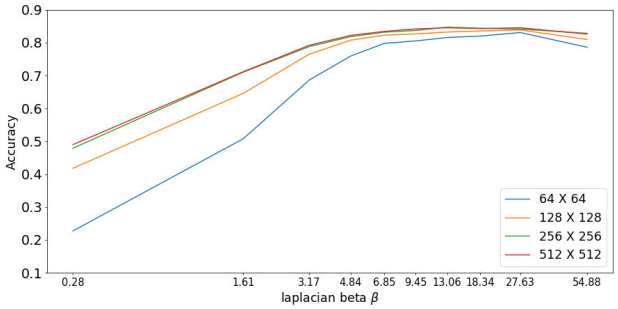


e. Accuracy of RAISE $256 \times 256$ test set at varying of training set

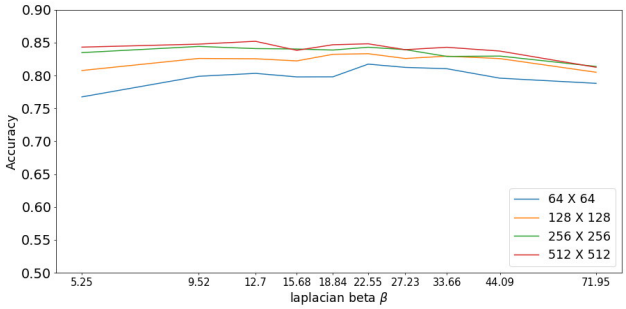


f. Accuracy of UCID $256 \times 256$ test set at varying of training set

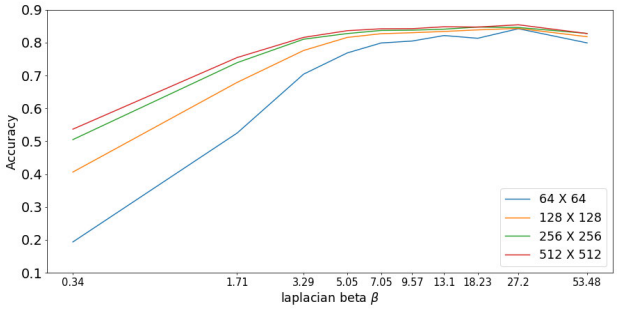


g. Accuracy of RAISE $512 \times 512$ test set at varying of training set

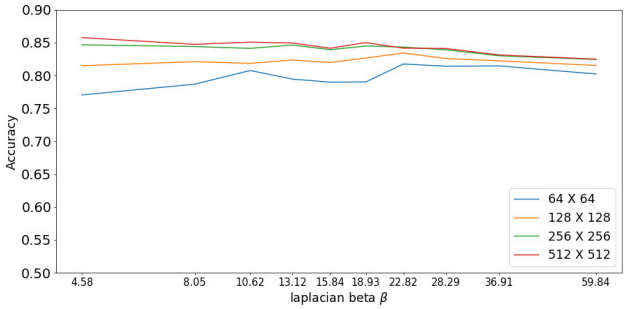


h. Accuracy of UCID $512 \times 512$ test set at varying of training set

**FIGURE 8. Accuracy of tests conducted on different test sets grouped and sorted by Laplacian $\beta$, shown on a logarithmic scale. It is worth noting that, given a patch size $N \times N$, the same dataset was employed as reference (i.e., RAISE $N \times N$) for both input (i.e., RAISE $N \times N$, UCID $N \times N$).**

greater than a $256 \times 256$ patch extracted from a RAISE [33] image ($\approx$5000 $\times$ 3000).

### C. CROSS DCT IMPLEMENTATION ANALYSIS

Recent works in literature analyse the effect of different Discrete Cosine Transform implementations in the final JPEG image generation [38]. To further validate our method a cross JPEG implementation test was conducted through the use of different types of DCTs. We employed Pillow and libjpeg-turbo[2] to compress the input images. The test's dataset is composed by 2000 RAISE images cropped $64 \times 64$ and

[2]https://github.com/libjpeg-turbo/libjpeg-turbo/

compressed two times with the aforementioned JPEG implementations. The results in Table 4 confirmed the overall robustness of the method also w.r.t different DCT implementations.

### D. CROSS PATCH SIZE ANALYSIS

It is worth noting that in all the experiments performed in the previous sections, once a specific patch size $N \times N$ has been chosen for the considered scenario, both training and test sets have been generated starting from patches of the same size. As already shown in Fig. 7 and Table 3 bigger patch sizes, due to the higher information content, provide better results. In this section we try to verify if it is possible to exploit, also partially, information contained in patches of different size with respect to the analyzed ones. Specifically cross patch size tests considering 8 datasets built from RAISE and UCID image collections have been conducted. Every test was done employing 1000 random images, compressed two times with $QF_1 \in \{55, 60, 65, 70, 75, 80, 85, 90, 95, 98\}$, $QF_2 = 90$ and patch sizes $64\times64$, $128\times128$, $256\times256$, $512\times512$. Test images have been then compared with four different training datasets obtained from RAISE images employing double compression with $Q_1$ and $Q_2$ constant quantization matrices and patch sizes $64 \times 64$, $128 \times 128$, $256 \times 256$, $512 \times 512$.

**TABLE 5. Accuracies obtained for every couple test/training with RAISE as test dataset.**

| Test \ Training | 64 | 128 | 256 | 512 |
|---|---|---|---|---|
| 64 | 0.677 | 0.699 | **0.703** | 0.699 |
| 128 | 0.698 | 0.744 | 0.758 | **0.760** |
| 256 | 0.705 | 0.758 | 0.780 | **0.783** |
| 512 | 0.710 | 0.768 | 0.792 | **0.801** |

As reported in Table 5 and 6, training datasets built from higher patch size work better. To understand how these improvements are related to the information content, the accuracy of AC coefficient estimation in all the considered scenarios (i.e., all combinations of training and test patch sizes) at varying of $\beta$ (eq. (1)) was studied. Although exploiting training datasets with bigger patch sizes always provides better results (see Fig. 8), the gain in terms of accuracy is higher when low $\beta$ values are considered (i.e., lower informative patches). This behavior is more evident in the experiments conducted on RAISE dataset (with respect to UCID) due to the different resolution of the original images used to extract patches. AC distributions with low $\beta$ values have almost all bins close to zero and is pretty difficult to discriminate among ones obtained with different first quantization factors. This is even worse when a limited number of elements are used to build these histograms. Such as example histograms generated from $64\times64$ and $512\times512$ patches have been obtained considering 64 and 4096 elements respectively. Higher patch sizes allow then, especially when the information content is limited, to better discriminate similar distributions.

**TABLE 6. Accuracies obtained for every couple test/training with UCID as test dataset.**

| Test \ Training | 64 | 128 | 256 | 512 |
|---|---|---|---|---|
| 64 | 0.754 | 0.770 | 0.775 | **0.777** |
| 128 | 0.789 | 0.812 | 0.824 | **0.829** |
| 256 | 0.799 | 0.824 | 0.837 | **0.843** |
| 512 | 0.799 | 0.824 | 0.842 | **0.846** |

## VII. CONCLUSION

First Quantization Estimation (FQE) is an important task in forensic investigation activities. We designed a method able to estimate the first quantization factors for JPEG double compressed images. One of the main contributions of the proposed work was the way we deal with the big amount of data avoiding overfitting. Specifically, constant matrices $M_i$ permitted to uncouple $\{q1, q2\}$ and the use of $m$ and $\beta$, limiting the range of candidate histograms to be compared, makes the execution time acceptable. Experimental tests showed the goodness of the technique outperforming state-of-the-art results whereas the use of KNN (with $k = 1$) to learn the distribution has been effective. The generalization of the proposed method was demonstrated by the experimental results which shown clearly how, in the aligned scenario, the method works better than other solutions for both custom and standard tables, becoming a viable solution to be employed in real-case scenarios. Finally the results with different image sizes and the analysis conducted on their informative content suggested new points of view in order to improve and formalize the proposed method. The formalization would lead to possibility to further reduce the computational time and to conduct analysis about different inputs like resized and non-aligned images and different tasks like tampering detection/localization.

## REFERENCES

[1] O. Giudice, A. Paratore, M. Moltisanti, and S. Battiato, "A classification engine for image ballistics of social data," in *Proc. Int. Conf. Image Anal. Process. (ICIAP)*. Springer, 2017, pp. 625–636.
[2] H. Farid, "Digital image ballistics from JPEG quantization: A followup study," Dept. Comput. Sci., Dartmouth College, Hanover, NH, USA, Tech. Rep. TR2008-638, 2008.
[3] Z. Fan and R. L. de Queiroz, "Identification of bitmap compression history: Jpeg detection and quantizer estimation," *IEEE Trans. Image Process.*, vol. 12, no. 2, pp. 230–235, Feb. 2003.
[4] A. Piva, "An overview on image forensics," *ISRN Signal Process.*, vol. 2013, p. 22, Oct. 2013.
[5] L. Verdoliva, "Media forensics and deepfakes: An overview," *IEEE J. Sel. Topics Signal Process.*, vol. 14, no. 5, pp. 910–932, Aug. 2020.

[6] O. Giudice, F. Guarnera, A. Paratore, and S. Battiato, "1-D DCT domain analysis for JPEG double compression detection," in *Proc. Int. Conf. Image Anal. Process. (ICIAP)*. Springer, 2019, pp. 716–726.

[7] E. Kee, M. K. Johnson, and H. Farid, "Digital image authentication from JPEG headers," *IEEE Trans. Inf. Forensics Security*, vol. 6, no. 3, pp. 1066–1075, Sep. 2011.

[8] M. C. Stamm, M. Wu, and K. J. R. Liu, "Information forensics: An overview of the first decade," *IEEE Access*, vol. 1, pp. 167–200, 2013.

[9] E. Y. Lam and J. W. Goodman, "A mathematical analysis of the DCT coefficient distributions for images," *IEEE Trans. Image Process.*, vol. 9, no. 10, pp. 1661–1666, 2000.

[10] T. H. Thai, R. Cogranne, and F. Retraint, "Statistical model of quantized DCT coefficients: Application in the steganalysis of jsteg algorithm," *IEEE Trans. Image Process.*, vol. 23, no. 5, pp. 1980–1993, May 2014.

[11] T. H. Thai, R. Cogranne, F. Retraint, and T.-N.-C. Doan, "JPEG quantization step estimation and its applications to digital image forensics," *IEEE Trans. Inf. Forensics Security*, vol. 12, no. 1, pp. 123–133, Jan. 2017.

[12] S. Battiato, O. Giudice, F. Guarnera, and G. Puglisi, "In-depth DCT coefficient distribution analysis for first quantization estimation," in *Proc. IEEE Int. Conf. Image Process. (ICIP)*, 2020, pp. 843–847.

[13] B. Li, T.-T. Ng, X. Li, S. Tan, and J. Huang, "Statistical model of JPEG noises and its application in quantization step estimation," *IEEE Trans. Image Process.*, vol. 24, no. 5, pp. 1471–1484, May 2015.

[14] J. Yang, Y. Zhang, G. Zhu, and S. Kwong, "A clustering-based framework for improving the performance of JPEG quantization step estimation," *IEEE Trans. Circuits Syst. Video Technol.*, vol. 31, no. 4, pp. 1661–1672, Apr. 2021.

[15] T. Bianchi and A. Piva, "Image forgery localization via block-grained analysis of JPEG artifacts," *Proc. IEEE Trans. Inf. Forensics Security*, vol. 7, no. 3, pp. 1003 –1017, Jun. 2012.

[16] T. Bianchi, A. De Rosa, and A. Piva, "Improved DCT coefficient analysis for forgery localization in JPEG images," in *Proc. IEEE Int. Conf. Acoust., Speech Signal Process. (ICASSP)*, May 2011, pp. 2444–2447.

[17] T. Bianchi and A. Piva, "Detection of non-aligned double JPEG compression with estimation of primary compression parameters," in *Proc. 18th IEEE Int. Conf. Image Process.*, Sep. 2011, pp. 1929–1932.

[18] F. Galvan, G. Puglisi, A. R. Bruna, and S. Battiato, "First quantization matrix estimation from double compressed JPEG images," *IEEE Trans. Inf. Forensics Security*, vol. 9, no. 8, pp. 1299–1310, Aug. 2014.

[19] N. Dalmia and M. Okade, "First quantization matrix estimation for double compressed JPEG images utilizing novel DCT histogram selection strategy," in *Proc. 10th Indian Conf. Comput. Vis., Graph. Image Process.* , 2016, pp. 1–8.

[20] H. Yao, H. Wei, T. Qiao, and C. Qin, "JPEG quantization step estimation with coefficient histogram and spectrum analyses," *J. Vis. Commun. Image Represent.*, vol. 69, May 2020, Art. no. 102795.

[21] N. Dalmia and M. Okade, "Robust first quantization matrix estimation based on filtering of recompression artifacts for non-aligned double compressed JPEG images," *Signal Process., Image Commun.*, vol. 61, pp. 9–20, Feb. 2018.

[22] F. Xue, Z. Ye, W. Lu, H. Liu, and B. Li, "MSE period based estimation of first quantization step in double compressed JPEG images," *Signal Process., Image Commun.*, vol. 57, pp. 76–83, Sep. 2017.

[23] T. H. Thai and R. Cogranne, "Estimation of primary quantization steps in double-compressed JPEG images using a statistical model of Discrete Cosine Transform," *IEEE Access*, vol. 7, pp. 76203–76216, 2019.

[24] J. Lukáš and J. Fridrich, "Estimation of primary quantization matrix in double compressed JPEG images," in *Proc. Digit. Forensic Res. Workshop*, 2003, pp. 5–8.

[25] G. Varghese and A. Kumar, "Detection of double JPEG compression on color image using neural network classifier," *Int. J. Innov. Res. Sci. Technol.*, vol. 3, no. 3, pp. 175–181, 2016.

[26] M. Barni, L. Bondi, N. Bonettini, P. Bestagini, A. Costanzo, M. Maggini, B. Tondi, and S. Tubaro, "Aligned and non-aligned double JPEG detection using convolutional neural networks," *J. Vis. Commun. Image Represent.*, vol. 49, pp. 153–163, Nov. 2017.

[27] I. Amerini, T. Uricchio, L. Ballan, and R. Caldelli, "Localization of JPEG double compression through multi-domain convolutional neural networks," in *Proc. IEEE Conf. Comput. Vis. Pattern Recognit. Workshops (CVPRW)*, Jul. 2017, pp. 53–59.

[28] Q. Wang and R. Zhang, "Double JPEG compression forensics based on a convolutional neural network," *EURASIP J. Inf. Secur.*, vol. 2016, no. 1, p. 23, Dec. 2016.

[29] Y. Niu, B. Tondi, Y. Zhao, and M. Barni, "Primary quantization matrix estimation of double compressed JPEG images via CNN," *IEEE Signal Process. Lett.*, vol. 27, pp. 191–195, Jun. 2020.

[30] B. Tondi, A. Costranzo, D. Huang, and B. Li, "Boosting CNN-based primary quantization matrix estimation of double JPEG images via a classification-like architecture," 2020, *arXiv:2012.00468*. [Online]. Available: http://arxiv.org/abs/2012.00468

[31] G. K. Wallace, "The JPEG still picture compression standard," *Commun. ACM*, vol. 34, no. 4, pp. 30–44, Apr. 1991.

[32] J. Park, D. Cho, W. Ahn, and H. Lee, "Double JPEG detection in mixed JPEG quality factors using deep convolutional neural network," in *Proc. Eur. Conf. Comput. Vis. (ECCV)*, Sep. 2018, pp. 636–652.

[33] D.-T. Dang-Nguyen, C. Pasquini, V. Conotter, and G. Boato, "RAISE: A raw images dataset for digital image forensics," in *Proc. 6th ACM Multimedia Syst. Conf.*, Mar. 2015, pp. 219–224.

[34] D. Ravì, G. Farinella, V. Tomaselli, M. Guarnera, and S. Battiato, "Representing scenes for real-time context classification on mobile devices," *Pattern Recognit.*, vol. 48, p. 4, Oct. 2015.

[35] X. Hou, J. Harel, and C. Koch, "Image signature: Highlighting sparse salient regions," *IEEE Trans. Pattern Anal. Mach. Intell.*, vol. 34, no. 1, pp. 194–201, Jan. 2012.

[36] S. Battiato, O. Giudice, F. Guarnera, and G. Puglisi, "Computational data analysis for first quantization estimation on JPEG double compressed images," in *Proc. 25th Int. Conf. Pattern Recognit. (ICPR)*, Jan. 2021, pp. 5951–5958.

[37] G. Schaefer and M. Stich, "UCID: An uncompressed color image database," *Proc. SPIE*, vol. 5307, pp. 472–480, Dec. 2003.

[38] S. Agarwal and H. Farid, "Photo forensics from JPEG dimples," in *Proc. IEEE Workshop Inf. Forensics Secur. (WIFS)*, Dec. 2017, pp. 1–6.

**SEBASTIANO BATTIATO** (Senior Member, IEEE) received the degree *(summa cum laude)* in computer science from the University of Catania, in 1995, and the Ph.D. degree in computer science and applied mathematics from the University of Naples, in 1999. From 1999 to 2003, he was the Leader of the "Imaging" Team, STMicroelectronics, Catania. He joined the Department of Mathematics and Computer Science, University of Catania, as an Assistant Professor, an Associate Professor, and a Full Professor, in 2004, 2011, and 2016, respectively. He is currently a Full Professor of computer science with the University of Catania, where he is also the Scientific Coordinator of the Ph.D. Program in computer science. He is involved in the research and directorship with the Image Processing Laboratory (IPLab). He coordinates IPLab's participates on large scale projects funded by national and international funding bodies and private companies. He is also the Director (and the Co-Founder) of the International Computer Vision Summer School (ICVSS). He has edited six books and coauthored about 250 articles in international journals, conference proceedings, and book chapters. He is a co-inventor of 22 international patents. His current research interests include computer vision, imaging technology, and multimedia forensics. He has been a Regular Member of numerous international conference committees. He was a recipient of the 2017 PAMI Mark Everingham Prize for the series of annual ICVSS schools and the 2011 Best Associate Editor Award of the IEEE TRANSACTIONS ON CIRCUITS AND SYSTEMS FOR VIDEO TECHNOLOGY. He has been the Chair of several international events, including ICIAP 2017, VINEPA 2016, ACIVS 2015, VAAM 2014–2016, VISAPP 2012–2015, IWCV 2012, ECCV 2012, ICIAP 2011, ACM MiFor 2010–2011, and SPIE EI Digital Photography 2011–2013. He has been a Guest Editor of several special issues published in international journals. He is an Associate Editor of the *Journal of Electronic Imaging* (SPIE) and the *IET Image Processing Journal*.

**OLIVER GIUDICE** received the degree *(summa cum laude)* in computer engineering from the University of Catania, in 2011, and the Ph.D. degree in mathematics and computer science defending a thesis titled "Digital forensics ballistics: Reconstructing the source of an evidence exploiting multimedia data," in 2017. From 2011 to 2014, he was involved in various research projects at the University of Catania in collaboration with the Civil and Environmental Engineering Department and the National Sanitary System. In 2014, he started his job as a Researcher with the IT Department, Banca d'Italia. Since 2011, he collaborated with the IPLab, for various years, working on multimedia forensics topics and being involved in various forensics cases as a Digital Forensics Expert. Since 2016, he has been the Co-Founder of iCTLab s. r. l., spin-off of the University of Catania, company that works in the field of digital forensics, privacy and security consulting, and software development. His research interests include machine learning, computer vision, image coding, urban security, cryptocurrencies, and multimedia forensics.

**FRANCESCO GUARNERA** (Student Member, IEEE) received the bachelor's and master's degrees *(summa cum laude)* in computer science from the University of Catania, in 2009 and 2018, respectively. He is currently pursuing the Ph.D. degree with the University of Catania and ICT-Lab s. r. l. From 2009 to 2016, he was a Developer/Analyst/Project Manager of web applications based on Apache-MySql-PHP (AMP). He currently works on digital forensics and computer vision.

**GIOVANNI PUGLISI** received the M.S. degree *(summa cum laude)* in computer science engineering from Catania University, Catania, Italy, in 2005, and the Ph.D. degree in computer science, in 2009. From 2009 to 2014, he has worked with the University of Catania, Italy, as a Postdoctoral Researcher. He joined the Department of Mathematics and Computer Science, University of Cagliari, as an Associate Professor, in 2014. His research interests include image/video enhancement and processing, camera imaging technology, and multimedia forensics. He edited one book, coauthored more than 50 articles in international journals, conference proceedings, and book chapters. He is a co-inventor of several patents and serves as a Reviewer for different international journals and conferences.